CONF-860605--9

CONF-860605--9

DE86 008234

THE EFFECT OF NEUTRON IRRADIATION ON THE TENSILE PROPERTIES AND MICROSTRUCTURE OF SEVERAL VANADIUM ALLOYS*

D. N. Braski
Metals and Ceramics Division, Oak Ridge National Laboratory
Oak Ridge, TN 37831

ABSTRACT: Specimens of V–15Cr–5Ti, VANSTAR-7, and V–3Ti–1Si were encapsulated in TZM tubes containing ^{7}Li to prevent interstitial pickup and irradiated in FFTF (MOTA experiment) to a damage level of 40 dpa. The irradiation temperatures were 420, 520, and 600°C. For a better simulation of fusion reactor conditions, helium was preimplanted in some specimens using a modified version of the "tritium trick." The V–15Cr–5Ti alloy was most susceptible to irradiation hardening and helium embrittlement, followed by VANSTAR-7 and V–3Ti–1Si. VANSTAR-7 exhibited a relatively high maximum void swelling of ~6% at 520°C while V–15Cr–5Ti and V–3Ti–1Si had values of less than 0.3% at all three temperatures. The V–3Ti–1Si clearly outperformed the other two vanadium alloys in resisting the effects of neutron irradiation.

KEY WORDS: Vanadium alloys, neutron irradiation, irradiation hardening, helium embrittlement, void swelling

---

*Research sponsored by the Office of Fusion Energy, U.S. Department of Energy, under Contract No. DE-AC05-84OR21400 with the Martin Marietta Energy Systems, Inc.

INTRODUCTION

Vanadium alloys are currently being evaluated for use in fusion reactor first wall/blanket applications. Their relatively high thermal conductivity and low thermal expansion properties create lower thermal stresses for a given heat flux than the stainless steels, and the vanadium alloys demonstrate good mechanical properties in the design temperature range [1]. The vanadium alloys also show: good compatibility with lithium (a proposed blanket material [1]), excellent resistance to void swelling [2], and very low residual radioactivity after irradiation. In the past, vanadium alloys have been neutron irradiated in several experiments by encapsulating specimens in tubes containing sodium or an inert gas to prevent interstitial pickup that can embrittle the material. Like the other refractory metals (e.g., Mo, Ta, and W), vanadium reacts readily with the elements C, N, and O, which occupy interstitial positions in the structure, and is embrittled. Unfortunately, these encapsulation techniques have not been effective in preventing interstitial pickup and/or the starting materials were contaminated to begin with. In the present experiment, an effort was made to eliminate the factor of interstitial contamination, especially by oxygen. This was accomplished by starting with well-characterized alloys exhibiting good ductility and encapsulating specimens in TZM tubes containing lithium. Unlike sodium, from which dissolved oxygen will be absorbed by the vanadium alloy [3], lithium will <u>remove</u> oxygen from the metal at elevated temperatures [4]. In addition, a number of encapsulated specimens were thermally aged in lithium at the same times and temperatures as their counterparts in the reactor. These aged controls allow clear differentiation between any effects on tensile properties or microstructures that might be caused by the elevated-temperature exposure (and possible contamination) and the effects of neutron irradiation. The effect of irradiation at 420, 520, and 600°C in the Fast Flux Test Facility (FFTF) on the tensile behavior and microstructure of V–15Cr–5Ti, VANSTAR-7, and V–3Ti–1Si was investigated. The effect of helium, preimplanted to levels of ~80 appm using a modified "tritium trick" technique [5], was also evaluated.

EXPERIMENTAL PROCEDURE

The three vanadium alloys used in this experiment were V–15Cr–5Ti, VANSTAR-7, and V–3Ti–1Si. The source, chemistry, and final annealing heat treatment for each alloy are listed in Table 1. Miniature tensile specimens (SS-3 type) with the configuration shown in Fig. 1 were machined from 0.76-mm-thick sheet of V–15Cr–5Ti and VANSTAR-7, and from 0.51-mm-thick sheet of V–3Ti–1Si. Disks (3-mm diameter) for examination by transmission electron microscopy (TEM) were punched from 0.25-mm sheet.

Some tensile specimens and disks were implanted with ~80 appm ^{3}He using a modified version of the tritium trick [5]. The tritium charging times and final ^{3}He contents for each alloy are also given in Table 1. The charging temperature, charging pressure, and pumpout temperature were 400°C, 5.5×10^{-4} Pa, and 600°C, respectively, for all three alloys.

Selected specimens were encapsulated at Westinghouse Hanford Company (WHC) in 0.525 mm outside diameter × 8.255 mm inside diameter × 38.1 mm long TZM subcapsules containing enriched 99.99% ^{7}Li [6]. The enriched ^{7}Li was used because the 7.5% ^{6}Li present in natural lithium would result in unacceptable levels of helium and tritium formation. Each subcapsule was loaded with nine SS-3 tensile specimens and nine disks. The subcapsules were irradiated in the FFTF, MOTA assembly at 420, 520, and 600°C to a fast fluence of ~7 × 10^{22} n/cm^2 and a nominal damage level of ~40 dpa. The results for a few specimens from cycle 4 (10 dpa at 420°C and 17 dpa at 520°C) will also be shown in this report [7]. An equal number of control specimens were also encapsulated in capsules with ^{7}Li and thermally aged for 257 days at the same three temperatures used in the irradiation.

Both irradiated and control tensile specimens were tested at the irradiation/aging temperature in a hot cell tensile machine under a reduced pressure of less than 10^{-4} Pa. The crosshead speed was 8.5 μm/s (strain rate = 1.1×10^{-3} s^{-1}). After testing, the fracture surfaces were examined using a scanning electron microscope (SEM) installed in a radioactive hot cell [8]. Microstructural details were studied by TEM using the irradiated disks that were subsequently electropolished in a solution of 1 part conc. H_2SO_4 to 7 parts methanol, at −30°C.

RESULTS

Tensile Tests

The results of tensile tests on the aged vanadium alloy control specimens and postirradiation tensile tests on the same alloys are listed in Tables 2 and 3, respectively.

V–15Cr–5Ti — The results of tensile tests conducted on the V–15Cr–5Ti alloy are shown graphically in Fig. 2. Typical stress-strain curves for specimens in various conditions are shown at the three irradiation temperatures. First, note that the thermally aged control specimens with or without the 74 appm of implanted helium exhibited tensile behavior that was virtually the same as the starting material. This establishes the technique of irradiating vanadium alloys in lithium as a viable one (i.e., the exposure to lithium did not affect the tensile properties).

Neutron irradiation hardened the material as shown by the marked increase in yield strengths and reduction in elongation. This was especially true at 420°C, where both implanted and unimplanted specimens failed at very low strains. However, at 520°C, most of the irradiated specimens demonstrated moderate ductility in spite of a doubling of their yield strengths. The irradiated specimen implanted with helium (I/40/74) displayed low ductility after 40 dpa. Serrated portions of the stress-strain curves were observed occasionally in tests conducted at 520°C, and frequently at 600°C. This phenomenon is not unusual for vanadium and its alloys and is probably due to dynamic strain aging [9]. Irradiation hardening was lower at 600°C than at the two lower temperatures as demonstrated by the specimen without helium (I/40/0) shown in the upper graph in Fig. 2. Two specimens that contained 74 appm He became very brittle after irradiation at 600°C and broke during subsequent handling.

<u>VANSTAR-7</u> — Typical stress-strain curves for the starting VANSTAR-7 material, aged controls, and irradiated specimens are presented in Fig. 3. As in the case of V—15Cr—5Ti, aging at the three elevated temperatures for 257 days had little effect on the tensile properties of VANSTAR-7. At 420°C, irradiation doubled the yield strength after 10 dpa and tripled it after 40 dpa. In spite of this tremendous hardening, the VANSTAR-7 specimen retained excellent ductility. Moreover, the ductility was unaffected by the implanted helium, at least at the levels investigated. At 520°C, the VANSTAR-7 specimens without helium exhibited total elongations of at least 4% in spite of even greater amounts of irradiation hardening (e.g., curves I/40/0 and I/17/0). However, unlike the results at 420°C, specimens containing helium showed signs of embrittlement (see curves I/40/70 and I/17/150).

At 600°C, irradiation hardening was attenuated and the specimen with 70 appm He (I/40/70) had a total elongation comparable to a similar specimen without helium (I/40/0). As before, serrated yielding was most evident at the higher temperature, but for some reason was not observed in the irradiated VANSTAR-7 specimens.

V—3Ti—1Si — Like the first two vanadium alloys, aged V—3Ti—1Si specimens demonstrated the same tensile behavior as the starting material (Fig. 4). Only one specimen, A/0 at 600°C, exhibited a noticeable difference in tensile behavior. The V—3Ti—1Si specimens also showed substantial irradiation hardening at 420°C, but unlike the VANSTAR-7 specimens, this hardening tended to saturate at the relatively low damage level of 10 dpa. Reasonable ductilities were exhibited by all of the irradiated specimens including those containing helium. However, the lower elongation exhibited by the specimen with the higher helium content (I/10/135) may be an indication that higher helium levels may not be accommodated very well At 520 and 600°C, the magnitude of irradiation hardening was markedly lower in the V—3Ti—1Si than the other two alloys and saturated quickly at relatively low damage levels. Along with the reduced hardening, the V—3Ti—1Si specimens exhibited total elongations that were usually above 10% and were quite insensitive to implanted helium.

Ductility — The effects of irradiation, irradiation temperature, and helium on the ductility of the three vanadium alloys are shown in Fig. 5, where total elongation is plotted as a function of temperature. Starting at the top of the figure with V—15Cr—5Ti, a small but consistent difference is seen between aged specimens containing helium and those without helium. The difference was probably caused by the slight hardening due to ^{3}He implantation and the introduction of small ^{3}He bubbles in the microstructure.

Irradiation to 40 dpa had a drastic effect on elongation at 420°C due to irradiation hardening that abated with increased irradiation temperatures. The V–15Cr–5Ti specimens were particularly sensitive to the presence of helium in the microstructure as relatively low elongations were measured in all of the irradiated specimens containing helium. Thermally aged VANSTAR-7 specimens also had slightly lower elongations at 420 and 520°C than those without helium, but this difference disappeared at 600°C. Irradiation hardening substantially lowered the ductility of VANSTAR-7 across the entire temperature range, but the effect of helium was less than observed for V–15Cr–5Ti. Finally, for V–3Ti–1Si, some large scatter in the results for the aged specimens with and without helium prohibits any conclusions to be made concerning helium and its effects on aged specimens. However, it is seen that both irradiation and helium had less effect on the ductility of V–3Ti–1Si specimens compared to those of the other alloys. Of the vanadium alloys tested, the V–3Ti–1Si alloy clearly had the best performance as far as postirradiation ductility is concerned.

Scanning Electron Microscopy

The results of the SEM examinations of irradiated vanadium alloys are given in Table 4. The type of fracture observed by SEM is listed for each alloy as a function of helium level, damage level, and irradiation temperature. These results couple directly with the stress-strain curves presented in Figs. 2–5 and help to identify the mechanism whereby each specimen failed. Note that eight representative micrographs have been selected from the table and are referenced in the table to the micrographs in Figs. 6 and 7.

V—15Cr—5Ti — Referring to Table 4, it is seen that V—15Cr—5Ti specimens, without helium and irradiated at 420°C, failed by a cleavage-type of fracture [Fig. 6(a)]. This suggests that irradiation hardening has elevated the yield strength of the material above the fracture (cleavage) stress, causing the material to fail transgranularly along cleavage planes. The "river" patterns on the cleavage faces [Fig. 6(a)] distinguish this type of fracture from intergranular, in which such patterns are missing from the exposed grain boundary surfaces [see Fig. 6(b)]. With 300 appm He, V—15Cr—5Ti specimens failed intergranularly after irradiation to 10 dpa at 420°C [Fig. 6(b)]. As will be shown later in TEM micrographs, helium bubbles formed in the grain boundaries and weakened them, thus causing intergranular failure (helium embrittlement) upon testing in tension. With less implanted helium and higher damage level (see 74 appm He in Table 4), the mechanisms of irradiation hardening and helium embrittlement overlap, producing a fracture surface characteristic of both (i.e., cleavage and intergranular separation), as shown in Fig. 6(c). For the V—15Cr—5Ti specimen conditions represented in this figure, the fraction of cleavage-type fracture outweighs that due to intergranular separation. At 520°C, 40 dpa, and 74 appm He, the situation was reversed (refer to Table 4) and the fracture mode was mostly intergranular with a small amount of cleavage as shown in Fig. 6(d). Three different fracture modes appeared after testing the specimen with 14 appm He, irradiated to 17 dpa at 520°C (see Table 4). Specimens of V—15Cr—5Ti without helium that were irradiated and tested at 520 and 600°C failed in a ductile manner and exhibited the familiar cone-like structure shown in Fig. 7(a).

VANSTAR-7 — All of the VANSTAR-7 specimens irradiated and tested at 420 and 600°C displayed ductile-type fracture surfaces similar to those shown in Fig. 7(a). At 520°C, irradiation to 40 dpa produced enough hardening in a specimen without helium to cause some cleavage fracture areas on a generally ductile surface [Fig. 7(b)]. Under these same conditions, a specimen with 70 appm He failed intergranularly as shown in Fig. 7(c), accounting for the low ductilities shown in Figs. 3 and 5. Intergranular fracture surfaces and some cleavage fracture were found at 17 dpa with 150 appm He.

V–3Ti–1Si — The relatively high ductility of this alloy demonstrated in the postirradiation tensile tests is also reflected in the results of the SEM examinations (Table 4). All of the irradiated V–3Ti–1Si specimens, with and without implanted helium, failed in a ductile manner. As an example, the ductile-type fracture surface of a specimen irradiated at 420°C without helium is shown in Fig. 7(d).

Transmission Electron Microscopy

The results of postirradiation tensile tests and SEM examinations support two mechanisms by which the vanadium alloys were embrittled by neutron irradiation: irradiation hardening and helium embrittlement. Before exploring a third source of material degradation — void swelling — it would be useful to correlate these two forms of embrittlement with the microstructure. The TEM micrographs in Fig. 8 show representative microstructures of the vanadium alloys that produced the three major types of tensile fracture observed: cleavage, intergranular separation, and ductile. Figure 8(a) shows the microstructure of V–15Cr–5Ti, without implanted helium, that was irradiated to 40 dpa at 420°C. Referring back to Figs. 2 and 5 (and Table 4), it is seen that this specimen failed at low strain with a cleavage mode of fracture. The microstructure in Fig. 8(a) is consistent with this mode of failure as it shows a high density of small dislocation loops and segments that are characteristic of irradiation hardening. There were no helium bubbles or voids observed in the structure. Figure 8(b) is a micrograph of the same alloy, with 300 appm He, that was irradiated to 17 dpa at 520°C and failed with only ~2% total elongation (see Fig. 5). It was not surprising that this specimen failed intergranularly along grain boundaries because it contained large helium bubbles.

The shape of many of the bubbles indicates that bubble coalescence had occurred at some stage of the experiment, probably during the tritium trick procedure itself. The ramifications of this result will be discussed later in this paper. Finally, a microstructure that effectively resisted both types of embrittlement and enabled the retention of good tensile ductility is shown in Fig. 8(c). It shows V—3Ti—1Si with 80 appm He after irradiation to 40 dpa at 600°C. A total elongation of ~12% was measured for this specimen tested at 600°C (Fig. 5). The microstructure is complex: large particles and extremely small helium bubbles in the grain boundaries, dislocation segments in the grain matrices, planar defects or precipitate phase with fringe contrast, an unknown phase with tiny bubbles attached, and a few voids.

Void Swelling — The microstructural response of the three vanadium alloys to irradiation-induced void swelling is summarized in Fig. 9. Representative electron micrographs are shown for each alloy at each of the three irradiation temperatures. In this figure, specimens containing

~80 appm He are compared. The micrographs were taken within grain matrices using absorption contrast imaging conditions and were used subsequently to calculate void swelling ($\Delta V/V$) [10]. Void swelling is observed to vary markedly with irradiation temperature. The actual swelling values are listed for irradiated specimens, with and without helium, in Table 3 and are shown graphically as a function of irradiation temperature in Fig. 10. The swelling behavior differs among the alloys. The peak swelling temperature for the highest swelling alloy, VANSTAR-7, was at 520°C while V–15Cr–5Ti had its highest swelling at 600°C. The V–3Ti–1Si specimens containing helium had a swelling minimum at 520°C, and specimens without helium showed no swelling at 600°C. Except for this last instance, the swelling in specimens without helium followed those containing helium in a parallel fashion and in all cases exhibited lower swelling values. Therefore, it was concluded that helium slightly enhanced void swelling. Finally, it should be emphasized that most of th. swelling values measured for the three vanadium alloys are really very low. The swelling data in Fig. 10 was plotted on a logarithmic scale, because it was well-behaved and illustrates some consistent effects of helium. However, this can also be misleading because the lower values are overemphasized. From a technological standpoint, it would have been better to use a linear scale for swelling. Then all but two or three points would drop to positions just slightly above zero swelling. Only the swelling values for VANSTAR-7 at 520°C (~1 and 6%) and perhaps the V–15Cr–5Ti specimens at 600°C (~0.3%) would be considered significant.

DISCUSSION

Helium Implantation

Helium must be preimplanted in vanadium alloys because nuclear reactors such as FFTF have neutron spectra that will not produce the helium expected in a fusion reactor. A fusion reactor will produce about 5 appm He/dpa [11]. Although the tritium trick has been used by a number of investigators to determine the effects of helium on metals [12,13], the present experiment may be one of the first where it has been utilized to preimplant helium prior to irradiation. Helium is usually implanted with a cyclotron. There are a number of advantages to using tritium rather than a cyclotron for injecting the helium. The tritium trick will implant ^{3}He uniformly on a macroscopic scale in large numbers of thick specimens that can be used to provide mechanical properties data. The cyclotron technique is capable of injecting very thin specimens (foils) and is very expensive. In the tritium trick, the tritium decay process can easily be conducted at elevated temperatures (the subsequent irradiation temperatures), making it a good simulation of processes occurring in a fusion reactor first wall. At the same time, the reader is reminded that this is probably more severe than actual service because implanted specimens start out with helium bubble distributions that may be representative of several years in the reactor. There are some additional concerns in using the tritium trick. First, tritium constitutes a slight radiation hazard and implanted specimens will usually contain small residual amounts of the isotope. They must be handled and stored in specified ways and tested in dedicated systems. Even more annoying is the fact that much of the ^{3}He is converted back to ^{3}H by neutron irradiation. At 40 dpa, only ~60% of the original ^3He is left in the specimen, even accounting for some retransformation of tritium back to ^3He (in a closed system) [14]. This last feature may also introduce small amounts of ^3He into unimplanted specimens sharing the same capsule. In spite of these drawbacks, the tritium trick appears to be a very convenient method of implanting helium in bulk specimens of vanadium alloys and it lends itself nicely for screening studies and alloy development.

Postirradiation Tensile Behavior

The main effects of neutron irradiation on the vanadium alloys studied are irradiation hardening, helium embrittlement, and void swelling. Although all three mechanisms are present through the range of experimental conditions used, one was usually prominent for any set of conditions. Irradiation hardening or irradiation embrittlement has been recognized for some time and is caused by the creation of dislocations, voids, and precipitate particles within the material. These imperfections resist the flow of dislocations through the structure during plastic deformation. Vanadium and other bcc metals already exhibit some unique tensile characteristics, such as yield point behavior, which is believed to be related to the interaction of dislocations with interstitial impurity elements such as C, N, and O. After irradiation, the concentration of defects in the microstructure increases radically, hardening the alloy. This is illustrated clearly in the stress-strain curves for all three alloys at 420 and 520°C as shown in Figs. 2 through 4. In the case of VANSTAR-7 at 420°C (Fig. 3), the amount of hardening was proportional to damage level with little sign of saturation, while at 520°C the hardening appears to have saturated by 40 dpa. The V–3Ti–1Si was most resistant to irradiation hardening (Fig. 4) as increases in yield strength were not as large and total elongations were greater. Furthermore, the hardening quickly saturated with increased damage level. The V–15Cr–5Ti specimens not only were hardened substantially, but at 420°C failed by cleavage at very low strains (Figs. 2 and 6; Table 4). For those specimens the stress needed to cause cleavage fracture (cleavage stress) was exceeded after very little deformation. At 520°C, the cleavage stress was not exceeded, but the specimen containing 74 appm He (curve I/40/74) failed prematurely by intergranular separation. In this instance, the hardening of the matrix and weakening of the grain boundaries by helium bubbles acted together, perhaps even synergistically, to reduce specimen ductility. At 600°C, some hardening was observed for V–15Cr–5Ti and VANSTAR-7 (Figs. 2 and 3), but very little hardening and excellent total elongation were exhibited by V–3Ti–1Si specimens with and without helium (Fig. 4). At this highest temperature, VANSTAR-7 specimens began to show some ductility problems (Fig. 3) that may have been related to their high swelling rather than hardening or helium, because the respective fracture surfaces were ductile (Table 4). The helium-implanted V–15Cr–5Ti specimens at 600°C suffered severe helium embrittlement and failed intergranularly during loading into the tensile machine chamber. However, the unimplanted specimen of the same alloy had excellent ductility (Fig. 2 — I/40/0).

Void Swelling

Both the V–15Cr–5Ti and V–3Ti–1Si were quite resistant to void swelling as shown in the micrographs in Fig. 9, graphically in Fig. 10, and in Table 3. On the other hand, VANSTAR-7 with 70 appm He demonstrated a

The V–15Cr–5Ti specimens in the X-287 experiment were sealed in sodium-filled capsules containing a zirconium getter material and were irradiated to 24 to 32 dpa at 400, 525, 625, and 700°C [16]. Some specimens were injected with ~80 appm He using a cyclotron. Some of the results for the X-287 experiment agree with the present work (i.e., effects of irradiation hardening and helium), but the starting material again showed total elongations that were one-half of the present heat. Therefore, all of the ductilities that could be compared directly were lower in the X-287 experiment. Although the precaution of using a getter material in the capsules was taken, the absence of thermally aged controls makes it difficult to assess the effectiveness of the getter in preventing specimen contamination.

The only results on irradiated VANSTAR-7 that could be found in the literature were by Bentley and Wiffen [18], who concentrated on microstructural changes and swelling. In that experiment, VANSTAR-7 was sealed in capsules under inert gas and irradiated to ~17 dpa in EBR-II at 496, 580, 690, and 805°C. The present results for swelling generally agree with those of Bentley and Wiffen, which showed that 496°C was the temperature of highest swelling for VANSTAR-7. The present irradiated microstructures of VANSTAR-7 at 520 and 600°C were also respectively similar to those irradiated in EBR-II at 496 and 580°C, except that the present void sizes and concentrations were larger for the higher damage level of 40 dpa.

Previous results on irradiated V–3Ti–1Si have been reported by Böhm [19]. Specimens were irradiated at 640°C in sodium-filled capsules to 1×10^{22} n/cm^2 (E > 0.1 MeV) in the BR-2 reactor in Möl/Belgium. Post-irradiation tensile tests showed a ~65% increase in yield strength at

650°C compared to the ~20% measured in this experiment at 600°C (compare results for V–3Ti–1Si in Tables 3 and 4). Böhm attributed the increase to irradiation as well as interstitial pickup in the surface regions of the specimens. The present results that show less total hardening at 600°C are consistent with those of Böhm in the sense that the component of hardening due to interstitial pickup was absent in the present specimens and total hardening would be expected to be less. It is interesting to note that the same planar imperfections or phase with stacking fault fringe contrast observed by Böhm [19] in the irradiated V–3Ti–1Si microstructures were also found in this experiment. More work is needed to prove that these imperfections are radiation-induced, as assumed by M. Bocek and J. O. Elen [20].

CONCLUSIONS

1. The tritium trick is an excellent technique for preimplanting helium in bulk specimens of vanadium alloys.

2. Vanadium alloys encapsulated in TZM tubes filled with ^{7}Li were protected from interstitial (C,N,O) pickup during irradiation.

3. The V–15Cr–5Ti alloy without preimplanted helium was most susceptible to irradiation hardening and failure by cleavage at 420°C. VANSTAR-7 was less susceptible and V–3Ti–1Si was least affected by this mechanism.

4. The V–15Cr–5Ti alloy was also more sensitive to helium embrittlement, followed by the VANSTAR-7 alloy, with V–3Ti–1Si showing the least sensitivity.

5. The VANSTAR-7 alloy exhibited a relatively high swelling value of nearly 6% at 520°C. V–15Cr–5Ti and V–3Ti–1Si were much more resistant to swelling and exhibited swelling values of less than 0.3% at all temperatures investigated.

6. The V–3Ti–1Si alloy performed better after irradiation in FFTF to 40 dpa than either V–15Cr–5Ti or VANSTAR-7. V–3Ti–1Si demonstrated excellent resistance to irradiation hardening, helium embrittlement, and void swelling.

ACKNOWLEDGMENTS

The author wishes to thank D. L. Smith, Argonne National Laboratory, R. E. Gold, Westinghouse Electric Corporation, and F. W. Wiffen and J. H. DeVan, Oak Ridge National Laboratory, for initial planning of the experiment. He also acknowledges D. Kaletta, KFK Karlsruhe, West Germany, for the V–3Ti–1Si material, A. M. Ermi, Westinghouse Hanford Corporation, for the encapsulations, B. M. Oliver, Rockwell International, for helium analyses, D. W. Ramey, for the tritium trick work, E. L. Ryan, N. H. Rouse, L. T. Gibson, and H. Blevins, for specimen preparation and testing, and Frances Scarboro, for manuscript preparation.

REFERENCES

[1] D. L. Smith, B. A. Loomis, and D. R. Diercks, J. Nucl. Mater., Vol. 135 (1985), pp. 125–137.

[2] B. A. Loomis, "Comparison of Swelling for Neutron and Ion-Irradiated MFE Structural Materials," ADIP Semiann. Prog. Rep. March 31, 1985, DOE/ER-0045/14, pp. 62–67.

[3] R. L. Klueh and J. H. DeVan, J. Less-Common Metals, Vol. 30 (1973), pp. 9–24.

[4] J. H. DeVan and R. L. Klueh, Nucl. Technol., Vol. 24 (Oct. 1974), pp. 64–72.

[5] D. N. Braski and D. W. Ramey, "A Modified Tritium Trick Technique for Doping Vanadium Alloys with Helium," 12th Inter. Symp. on Effects of Radiation on Materials, ASTM STP-870, F. A. Garner and J. S. Perrin, Eds., ASTM, Philadelphia, 1985, pp. 1211–1224.

[6] A. M. Ermi, "FFTF Fusion Irradiation, FFTF Cycles 4–6," ADIP Semiann. Prog. Rep. Sept. 30, 1984, DOE/ER-0045/13, pp. 21–40.

[7] D. N. Braski, "The Tensile Properties of Several Vanadium Alloys after Irradiation in FFTF," ADIP Semiann. Prog. Rep. March 31, 1985, DOE/ER-0045/4, pp. 54–61.

[8] J. R. Gibson and D. N. Braski, "Scanning Electron Microscope Facility for Examination of Radioactive Materials," ORNL/TM-9451 (February 1985).

[9] J. D. Baird, "The Effects of Strain-Aging Due to Interstitial Solutes on the Mechanical Properties of Metals," Metals and Materials, Vol. 5, Review No. 149 (February 1971), pp. 14–15.

[10] Annual Book of ASTM Standards, ASTM, Philadelphia, PA., E521-83 (1983), pp. 14–15.

[11] C. J. McHargue and J. L. Scott, Met. Trans. A, Vol. 9A (1978), pp. 151–159.

[12] J. F. Remark, A. B. Johnson, Jr., H. Farrar IV, and D. G. Atteridge, Nucl. Technol., Vol. 29 (1976), pp. 369–377.

[13] R. F. Mattas, H. Wiedersich, D. G. Atteridge, A. B. Johnson, Jr., and J. F. Remark, "Elevated-Temperature Tensile Properties of V–15Cr–5Ti Containing Helium Introduced by Ion Bombardment and Tritium Decay," Proc. 2nd Topical Meeting on the Technology of Controlled Nuclear Fusion, Richland, WA, Sept. 21–23, 1976, USERDA CONF-760935-P1, pp. 199–208.

[14] L. R. Greenwood, Argonne National Laboratory, private communication, July 19, 1983.

[15] R. Bajaj and R. E. Gold, "Evaluation of V–15Cr–5Ti Specimens after Neutron Irradiation in the MFE-2 Experiment," Phase I final report, Westinghouse Electric Corporation, Advanced Energy Systems Division, August 1983.

[16] M. L. Grossbeck and J. A. Horak, "Tensile Properties of Helium-Injected V–15Cr–5Ti after Irradiation in EBR-II," ADIP Semiann. Prog. Rep. Sept. 30, 1984, DOE/ER-0045/13, pp. 99–103.

[17] D. R. Diercks and D. L. Smith, "Environmental Effects on the Properties of Vanadium-Base Alloys," ADIP Semiann. Prog. Rep. March 31, 1985, DOE/ER-0045/14, pp. 179–180.

[18] J. Bentley and F. W. Wiffen, Nucl. Technol., Vol. 30 (1976), pp. 376–384.

[19] H. Böhm, "The Effect of Neutron Irradiation on the High-Temperature Mechanical Properties of Vanadium-Titanium Alloys," Proc. Intern. Conf. on Defects and Defect Clusters in B.C.C. Metals and Their Alloys, Gaithersburg, MD, August 1973, R. J. Arsenault, Ed., M. P. Graphics, Inc., Washington, D.C., pp. 163–175.

[20] M. Bocek and J. D. Elen, J. Nucl. Mater., Vol. 44 (1972), p. 194.

TABLE 1—Vanadium alloy data

Alloy	Heat	Composition, wt %								Final Heat Treatment	^3H Charging Time (h)	^3He Content[c] (appm)
		Cr	Ti	Fe	Zr	Si	C	O	N			
V—15Cr—5Ti[a]	CAM-834-3	14.5	6.2				0.032	0.031	0.046	1 h @ 1200°C	107	74
VANSTAR-7[a]	CAM-837-7	9.7		3.4	1.3		0.064	0.028	0.052	1 h @ 1350°C	206	70
V—3Ti—1Si[b]	11153		3.4	0.04		1.28	0.045	0.091	0.026	1 h @ 1050°C	67	82

[a]Source: Westinghouse Electric Corporation.
[b]Source: KFK, Karlsruhe, West Germany (Dr. D. Kaletta).
[c]Analyses performed by Dr. B. M. Oliver, Rockwell International Corporation, Canoga Park, CA.

TABLE 2—Results of tensile tests of vanadium control specimens aged 257 days in ^7Li

Specimen Number	Alloy	Helium Level (appm)	Aging/Test Temperature (°C)	Strength, MPa		Elongation, %	
				Yield	Ultimate Tensile	Uniform	Total
RD40	V—15Cr—5Ti	0	420	399	545	15.0	26.0
RD66	V—15Cr—5Ti	74	420	381	540	14.3	23.7
RA187	V—15Cr—5Ti	74	420	369	539	14.0	21.3
RD38	V—15Cr—5Ti	0	520	387	539	15.3	24.3
RA73	V—15Cr—5Ti	74	520	352	511	12.7	20.7
RA170	V—15Cr—5Ti	74	520	381	578	13.0	20.7
RD03	V—15Cr—5Ti	0	600	390	555	12.3	21.7
RA129	V—15Cr—5Ti	74	600	390	573	11.3	19.0
RA176	V—15Cr—5Ti	74	600	377	574	10.3	17.7
QA71	VANSTAR-7	0	420	256	398	16.0	26.3
QA73	VANSTAR-7	70	420	312	451	14.7	23.7
QA110	VANSTAR-7	70	420	302	448	12.7	22.3
QA08	VANSTAR-7	0	520	282	469	15.7	23.7
QA118	VANSTAR-7	70	520	283	469	13.0	20.7
QA119	VANSTAR-7	70	520	297	480	11.7	20.7
QA69	VANSTAR-7	0	600	298	490	12.3	20.0
QA80	VANSTAR-7	70	600	274	482	13.0	20.3
QA102	VANSTAR-7	70	600	261	473	14.0	22.0
RC54	V—3Ti—1Si	0	420	378	473	14.0	21.0
RC08	V—3Ti—1Si	82	420	444	550	10.7	17.3
RC42	V—3Ti—1Si	82	420	430	542	12.3	19.0
RC30	V—3Ti—1Si	0	520	454	595	11.0	20.0
RC33	V—3Ti—1Si	82	520	452	587	10.0	14.3
RC44	V—3Ti—1Si	82	520	446	570	14.0	20.0
RC55	V—3Ti—1Si	0	600	315	467	8.0	12.3
RC23	V—3Ti—1Si	82	600	300	495	13.3	20.0
RC57	V—3Ti—1Si	82	600	290	498	14.0	20.3

TABLE 3—Results of tensile tests and void swelling measurements for vanadium alloys irradiated to 40 dpa in FFTF(MOTA)

Specimen Number	Alloy	Helium Level (appm)	Irradiation/ Test Temperature (°C)	Strength, MPa		Elongation, %		Disk Number	ΔV/V (%)
				Yield	Ultimate Tensile	Uniform	Total		
RD14	V—15Cr—5Ti	0	420	825	913	0.8	0.8	RD18	0.003
RD64	V—15Cr—5Ti	74	420	--	793	0	0	RD52	0.005
RA34	V—15Cr—5Ti	74	420	692	834	0.8	0.8		
RD37	V—15Cr—5Ti	0	520	879	989	3.0	9.5	RD65	0.031
RA20	V—15Cr—5Ti	74	520	882	1003	1.8	1.8	RD38	0.046
RA108	V—15Cr—5Ti	74	520	868	956	1.5	1.7		
RD30	V—15Cr—5Ti	0	600	674	797	4.5	11.9	RD21	0.024
RA68	V—15Cr—5Ti	74	600	Broke during loading			--	RD16	0.283
RA139	V—15Cr—5Ti	74	600	Broke during loading			--		
QA19	VANSTAR-7	0	420	881	896	0.7	6.8	QB55	0.001
QA40	VANSTAR-7	70	420	978	997	0.9	6.0	QB38	0.004
QA71	VANSTAR-7	70	420	987	1002	0.6	5.7		
QA29	VANSTAR-7	0	520	1058	1138	1.5	4.0	QB60	0.958
QA87	VANSTAR-7	70	520	960	1016	1.3	1.3	QB39	5.940
QA91	VANSTAR-7	70	520	Failed at hole in shoulder					
QA53	VANSTAR-7	0	600	360	429	2.8	5.5	QB57	0.014
QA83	VANSTAR-7	70	600	651	755	3.2	4.5	QB40	0.065
QA90	VANSTAR-7	70	600	722	790	3.5	5.2		
RC34	V—3Ti—1Si	0	420	692	780	3.4	4.8	RC40	0.079
RC35	V—3Ti—1Si	82	420	795	884	3.8	6.0	RC18	0.090
RC53	V—3Ti—1Si	82	420	717	880	6.3	11.8		
RC17	V—3Ti—1Si	0	520	541	682	8.2	13.3	Disk lost	
RC11	V—3Ti—1Si	82	520	632	758	6.3	10.3	RC15	0.002
RC29	V—3Ti—1Si	82	520	565	688	6.0	10.9		
RC27	V—3Ti—1Si	0	600	378	564	8.1	12.1	R12	0
RC41	V—3Ti—1Si	82	600	276	480	7.8	11.3	RC11	0.052
RC43	V—3Ti—1Si	82	600	369	583	8.8	12.3		

TABLE 4—SEM Results

Alloy	Helium Level (appm)	420°C		520°C		620°C 40 dpa
		10 dpa	40 dpa	17 dpa	40 dpa	
V—15Cr—5Ti	0	Cleavage[a]	6A[b]/Cleavage	Ductile	Ductile	7[a]/ductile
V—15Cr—5Ti	14	—	—	Ductile + Cleavage + Intergranular	—	
V—15Cr—5Ti	74	—	6C/Cleavage + Intergranular	—	6d/Intergranular + some cleavage	Intergranular
V—15Cr—5Ti	300	6B/inter-granular	—	Intergranular	—	—
VANSTAR-7	0	Ductile	Ductile	Ductile	7b/ductile + cleavage	Ductile
VANSTAR-7	70	—	Ductile	—	7c/Intergranular	Ductile
VANSTAR-7	150	Ductile	—	Intergranular + some cleavage	—	—
V—3Ti—1Si	0	Ductile	7d/ductile	Ductile	Ductile	Ductile
V—3Ti—1Si	82	Ductile	—	Ductile	—	—
V—3Ti—1Si	135	Ductile	—	Ductile	—	—

[a]Broke in grips at ~100°C lower temperature.
[b]Alpha numeric designation is figure number of micrograph.

LIST OF FIGURES

ORNL- DWG 84-14010R

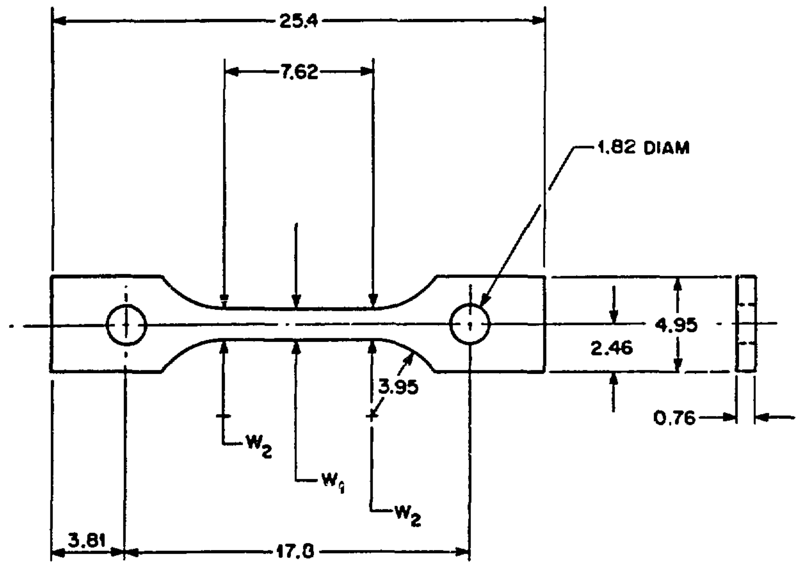

W1 = 1.52 mm
W2 = 0.025 TO 0.038 mm
GREATER THAN W1

DIMENSIONS IN MILLIMETERS

FIG. 1—SS-3 type sheet tensile specimen.

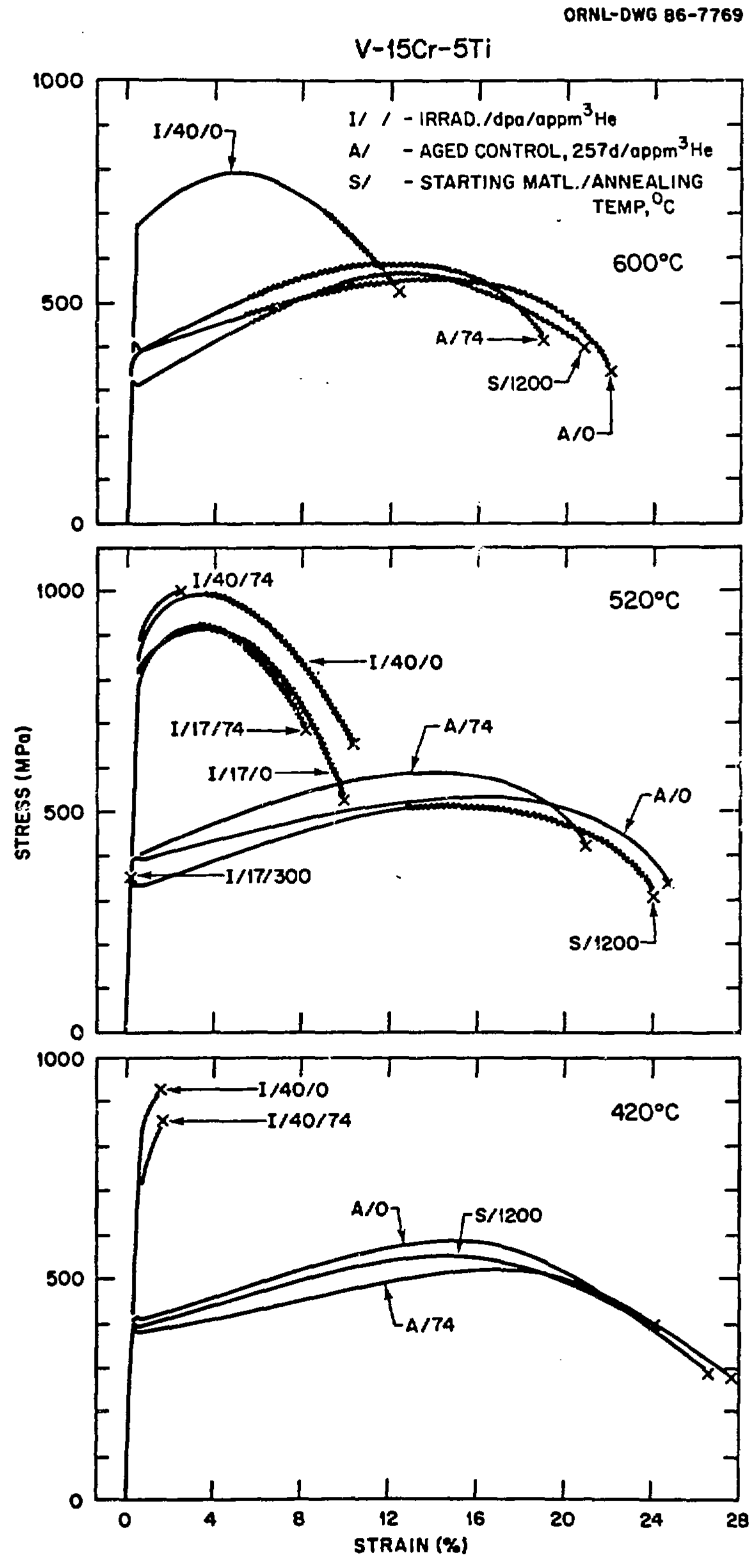

FIG. 2—Stress-strain curves for V—15Cr—5Ti alloy in the starting condition (s), after aging for 257 days in lithium (A), and after irradiation in FFTF(MOTA)—(I).

ORNL-DWG 86-7771

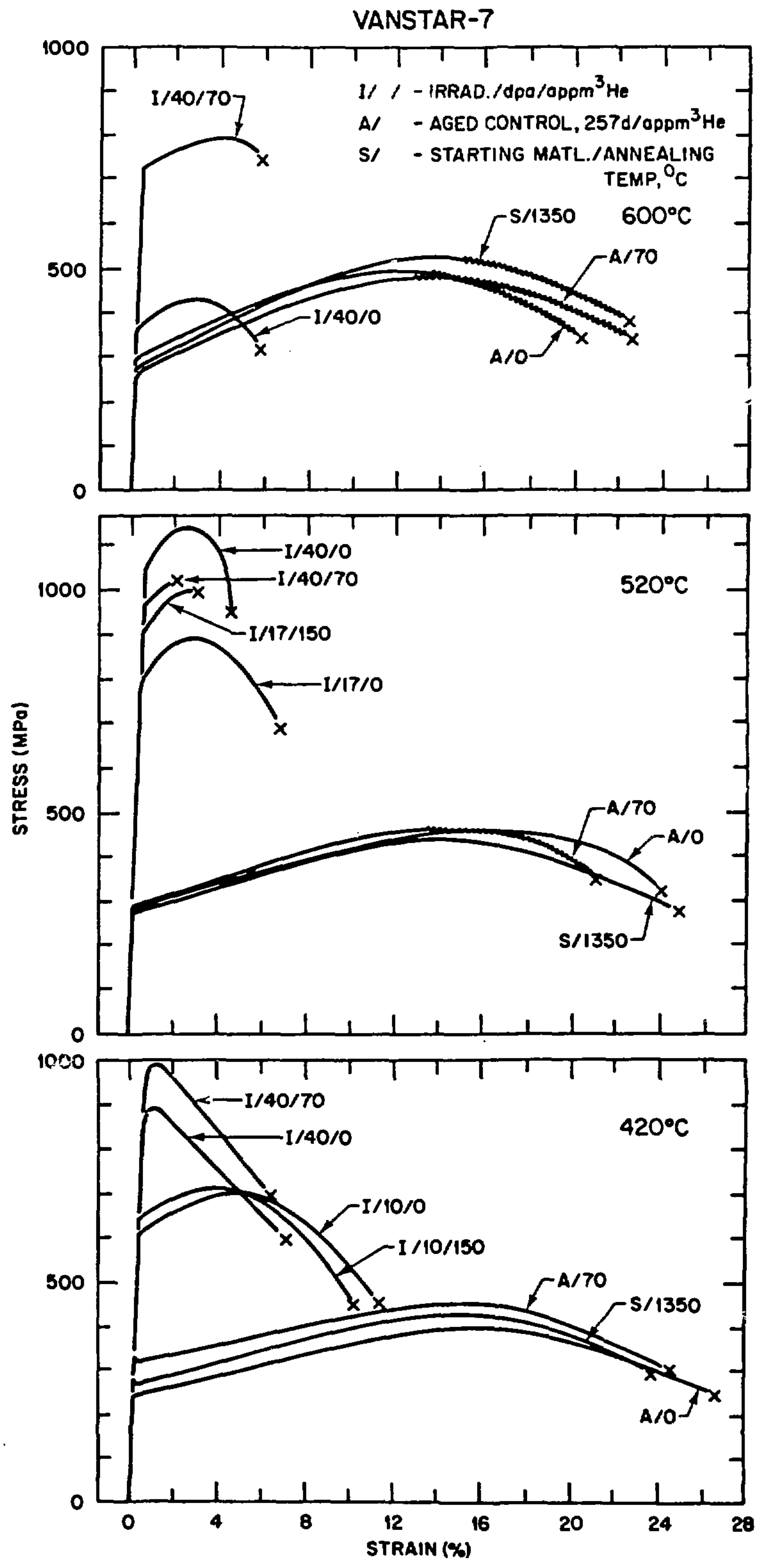

FIG. 3—Stress-strain curves for VANSTAR-7 alloy in the starting condition (S), after aging for 257 days in lithium (A), and after irradiation in FFTF(MOTA) — (I).

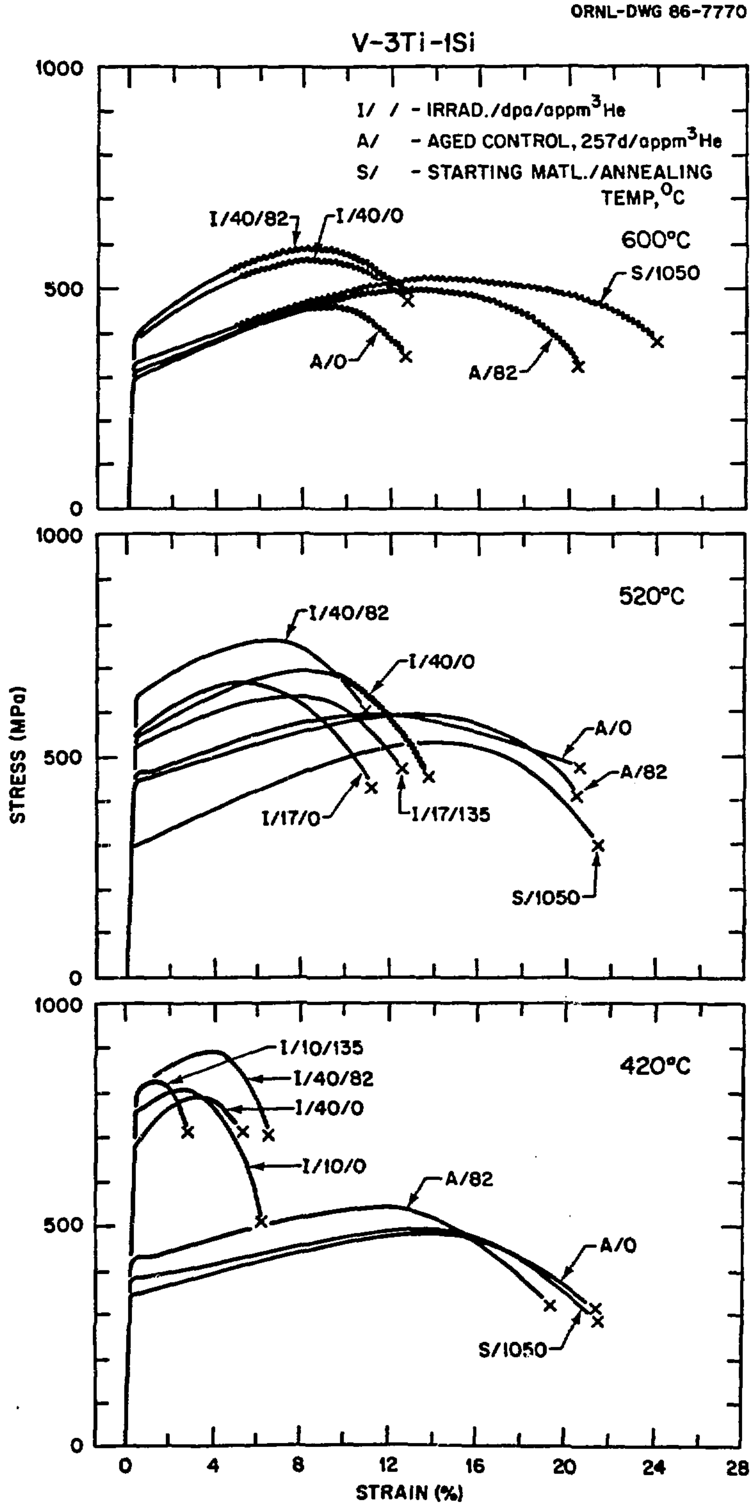

FIG. 4—Stress-strain curves for V-3Ti-1Si alloy in the starting condition (S), *after aging for 257 days in lithium* (A), and after irradiation in FFTF(MOTA) — (I).

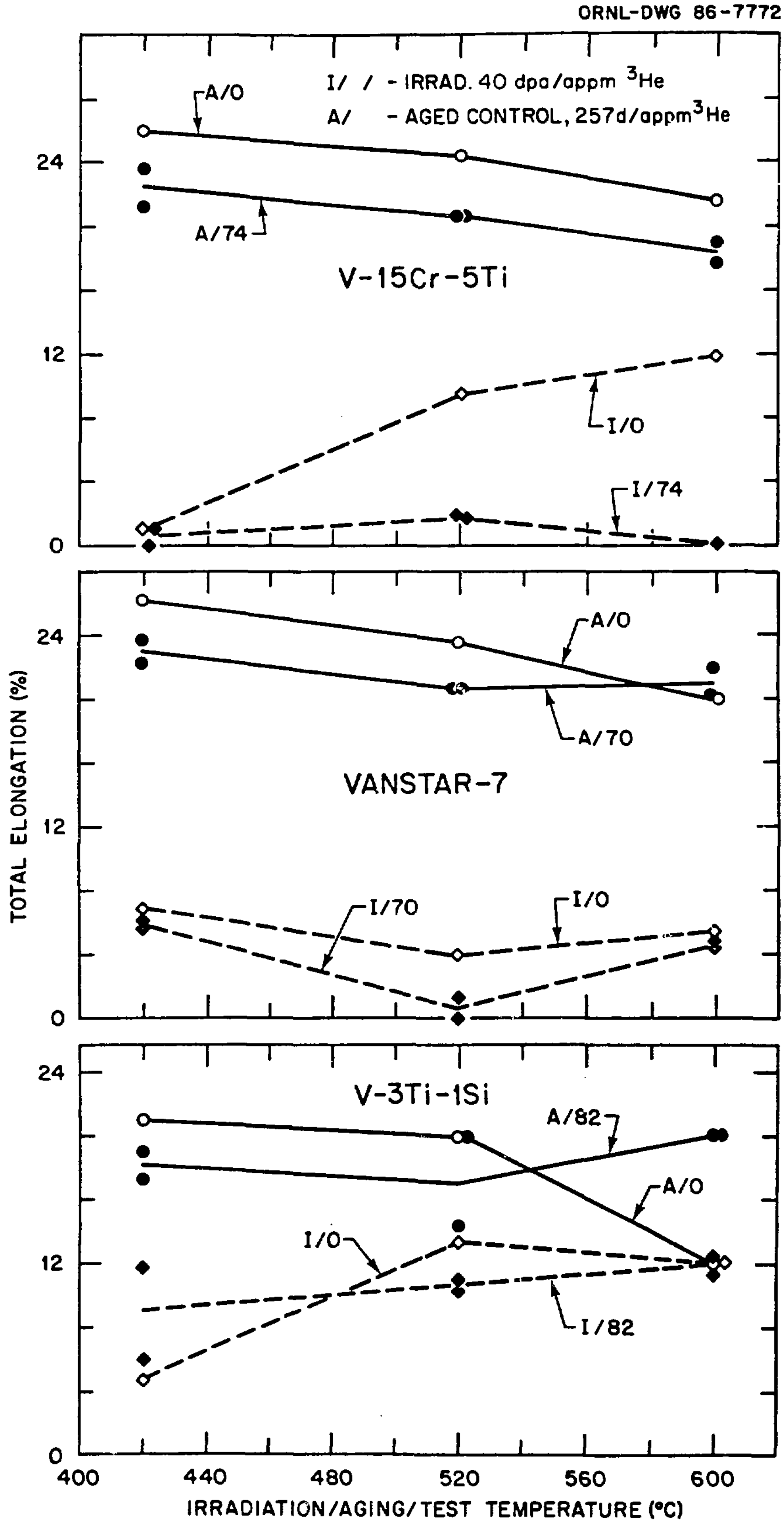

FIG. 5—Total elongation of vanadium alloy aged control specimens (A) and specimens irradiated in FFTF(MOTA) to 40 dpa (I) as a function of temperature.

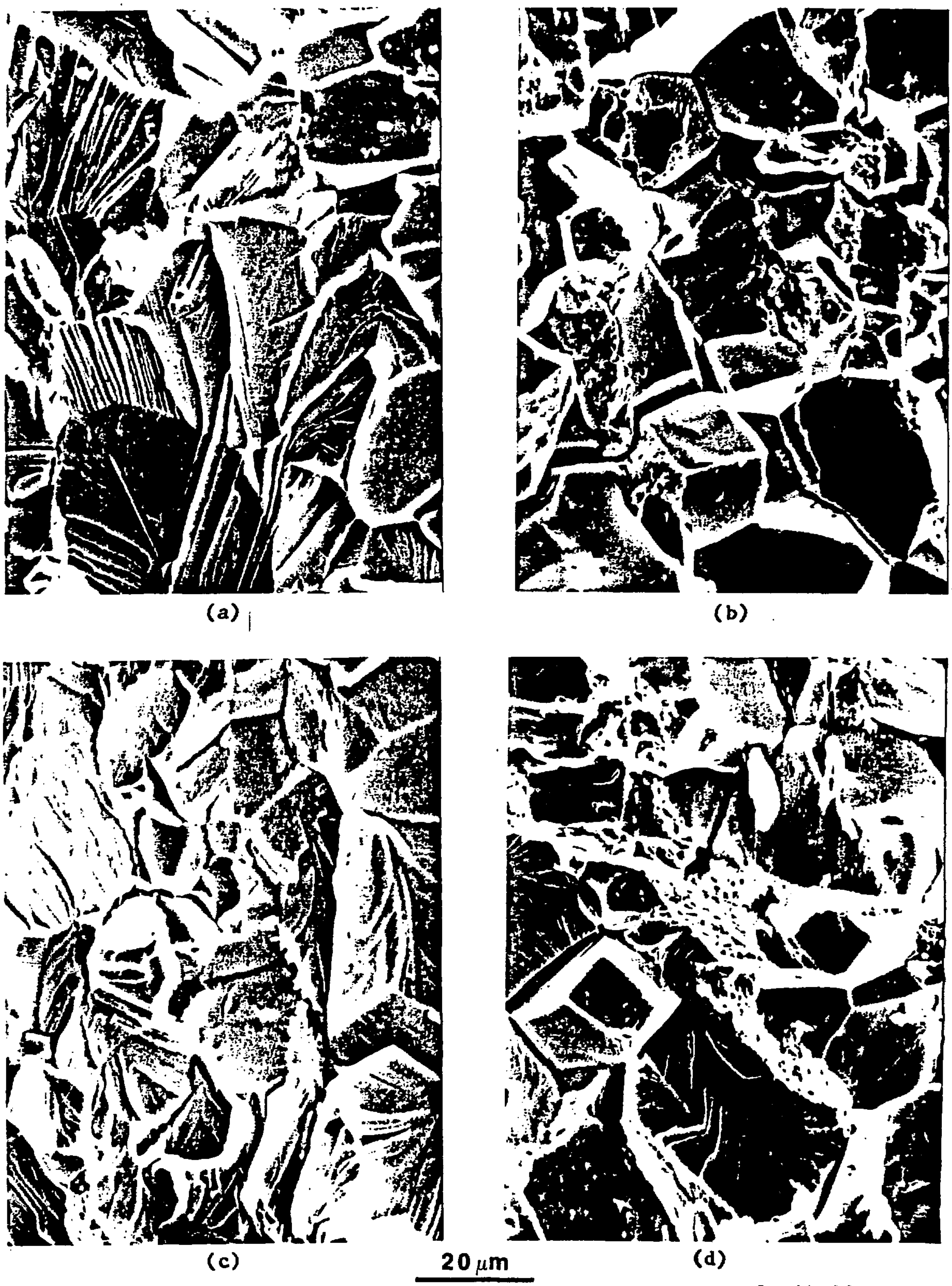

FIG. 6—Fractographs of V—15Cr—5Ti after irradiation in FFTF(MOTA) and tensile testing at the irradiation temperature (refer to Table 4).

(a) No helium, irradiated at 420°C to 40 dpa, cleavage.
(b) 300 appm He, irradiated at 420°C to 10 dpa, intergranular.
(c) 74 appm He, irradiated at 420°C to 40 dpa, cleavage to intergranular,
(d) 74 appm He, irradiated at 520°C to 40 dpa, intergranular plus cleavage

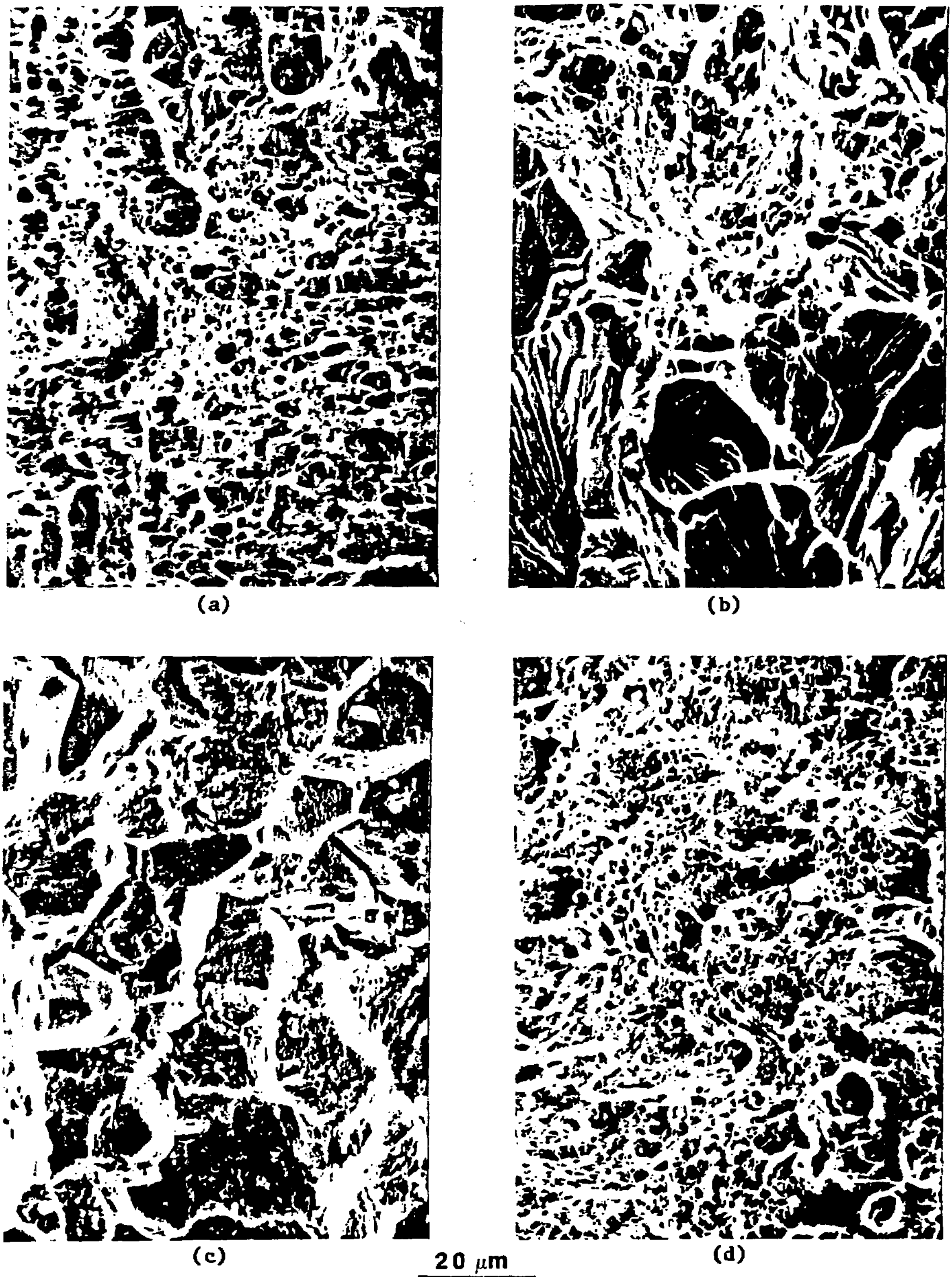

FIG. 7—Fractographs of vanadium alloys after irradiation in FFTF(MOTA) and tensile testing at the irradiation temperature (refer to Table 4).

(a) V—15Cr—5Ti, no helium, irradiated at 600°C to 40 dpa, ductile.
(b) VANSTAR-7, no helium, irradiated at 520°C to 40 dpa, ductile plus cleavage.
(c) VANSTAR-7, 70 appm He, irradiated at 520°C to 40 dpa, intergranular,
(d) V—3Ti—1Si, no helium, irradiated at 420°C to 40 dpa, ductile.

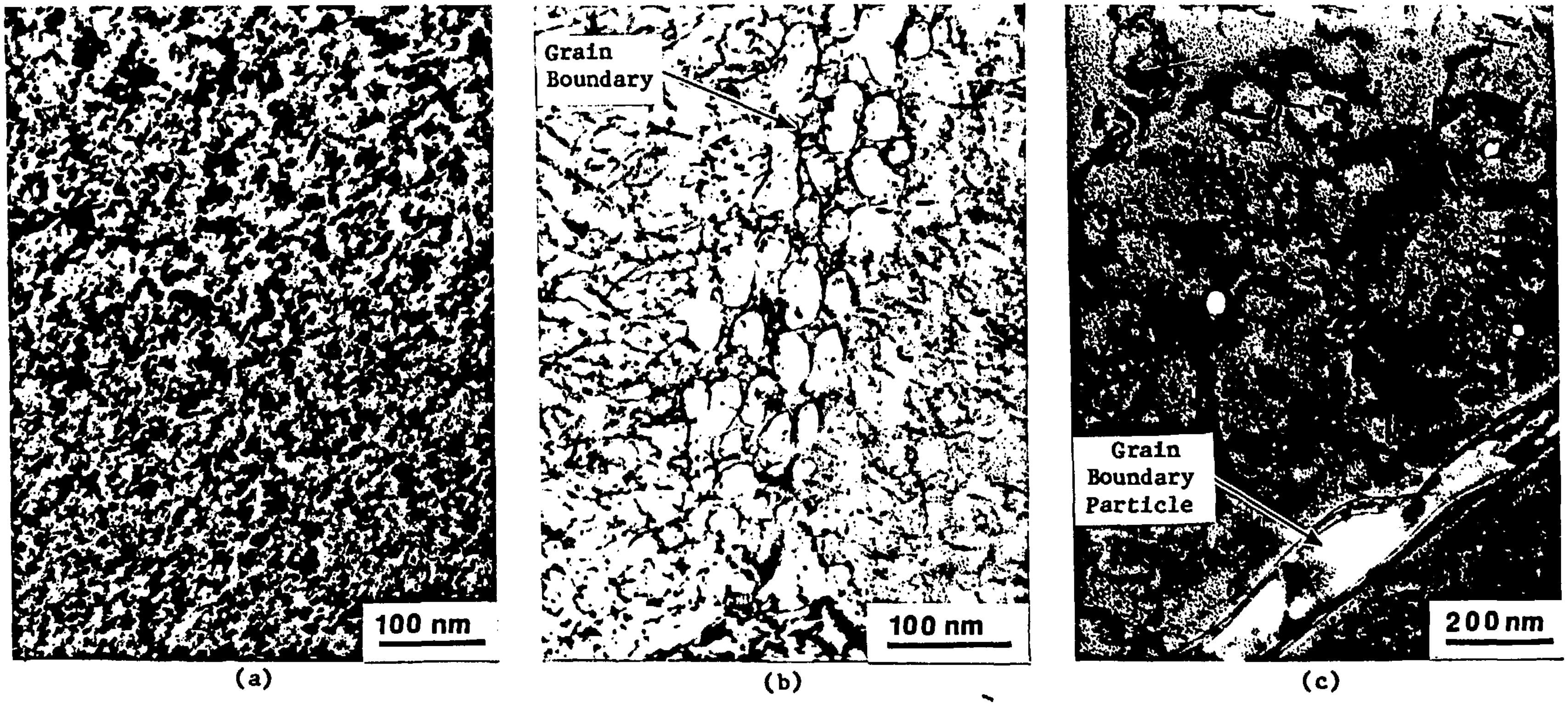

FIG. 8—Representative vanadium alloy microstructures for different tensile behavior and fracture modes.

(a) V—15Cr—5Ti, no helium, irradiated at 420°C to 40 dpa, cleavage fracture.
(b) V—15Cr—5Ti, 300 appm He, irradiated at 520°C to 17 dpa, intergranular fracture.
(c) V—3Ti—1Si, 82 appm He, irradiated at 600°C to 40 dpa, ductile fracture.

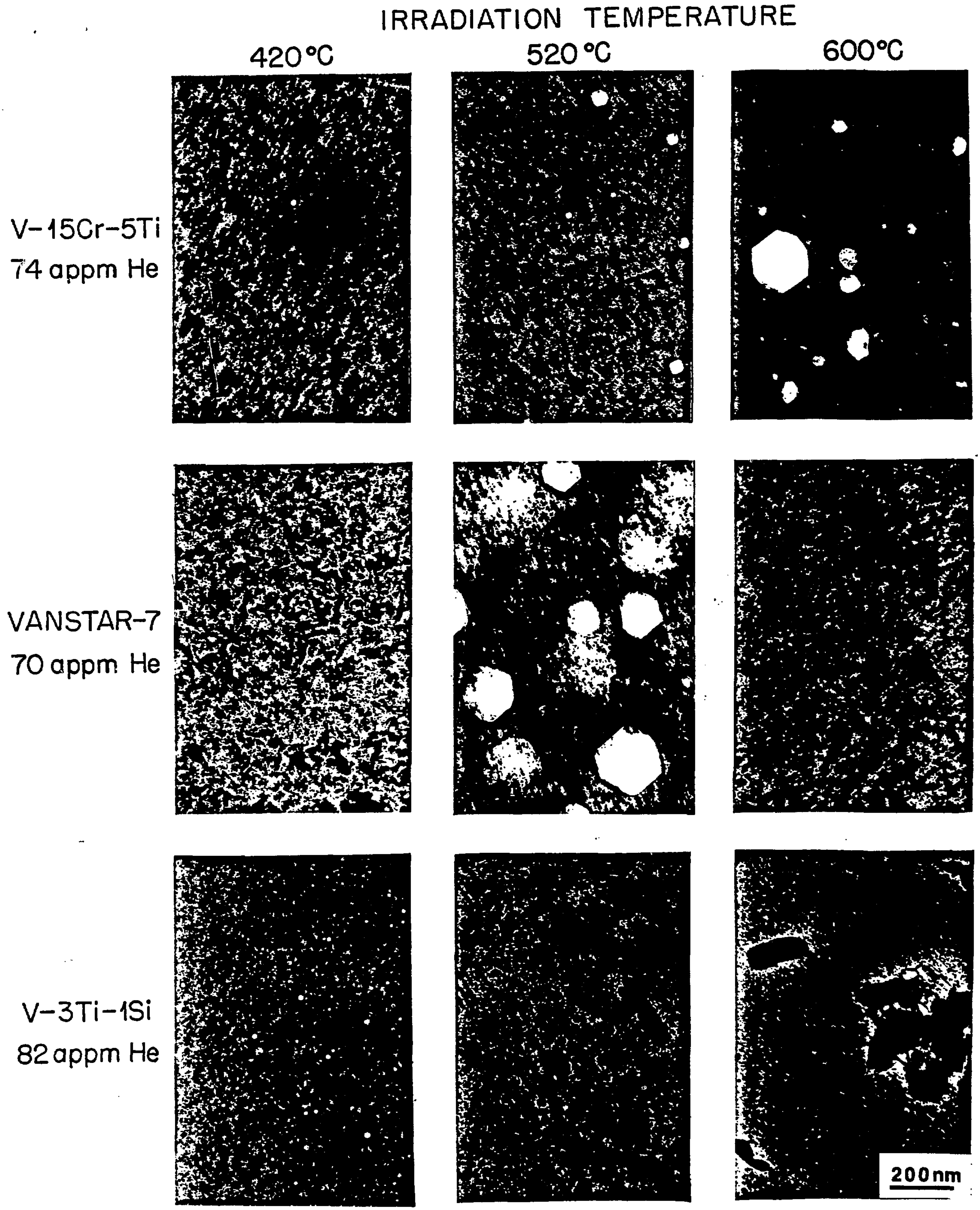

FIG. 9—Representative micrographs of vanadium alloys after irradiation in FFTF(MOTA) to 40 dpa showing irradiation-produced voids.

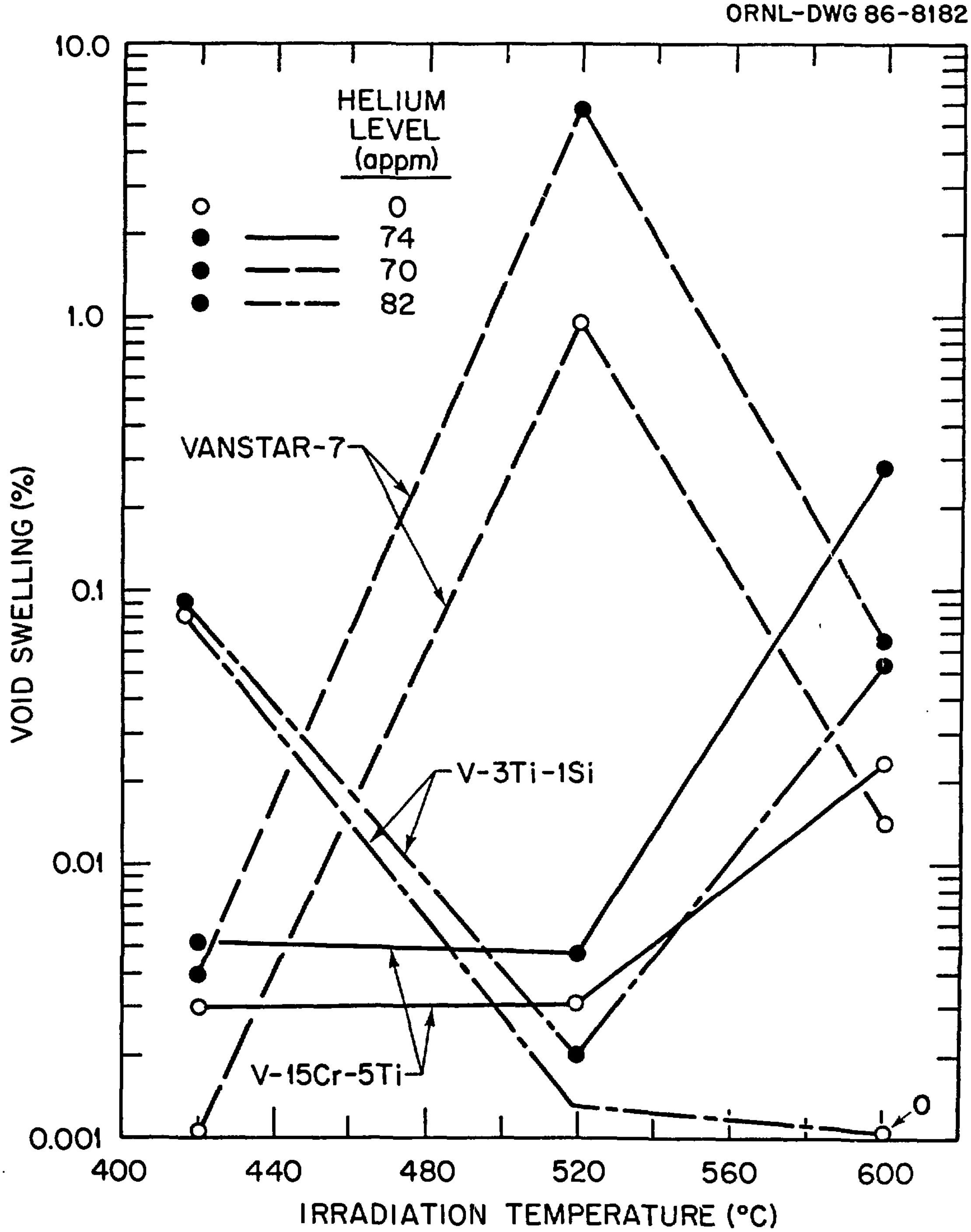

FIG. 10—Void swelling measured in vanadium alloys, with and without preimplanted helium, after irradiation in FFTF(MOTA) to 40 dpa. Note logarithmic scale for void swelling.